

A Numerical Scheme for Multi-fluid Magnetohydrodynamics

S. A. E. G. Falle

Department of Applied Mathematics, University of Leeds, Leeds LS2 9JT, UK.

31 October 2018

ABSTRACT

This paper describes a numerical scheme for multi-fluid hydrodynamics in the limit of small mass densities of the charged particles. The inertia of the charged particles can then be neglected, which makes it possible to write an evolution equation for the magnetic field that can be solved using an implicit scheme. This avoids the severe restriction on the stable timestep that would otherwise arise at high resolution, or when the Hall effect is large. Numerical tests show that the scheme can accurately model steady multi-fluid shock structures both with and without sub-shocks. Although the emphasis is on shocks in molecular clouds, a multi-dimensional version of this code could be applied to any Astrophysical flow in which ambi-polar diffusion or the Hall effect, or both play a significant role.

Key words: ISM: MHD - shock waves - dust, numerical methods, molecules.

1 INTRODUCTION

In dense molecular clouds, the density of charged particles can be so low that the scale on which ambi-polar resistivity becomes important cannot be assumed to be negligibly small. The most obvious effect of this is that it allows the existence of shock structures that are much thicker than those determined by viscous effects (see e.g. Draine & McKee 1993), but the enhanced magnetic diffusion also plays a role in the large scale dynamics of such clouds (see e.g. Mouschovias 1991).

The structure of shocks in which the dissipation is due to ambi-polar resistivity rather than viscosity has been studied extensively (e.g. Mullan 1971; Draine 1980; Flower, Pineau des Forêts & Hartquist 1985; ; Draine 1986; Wardle & Draine 1987; Chernoff 1987; Roberge & Draine 1990; Pilipp & Hartquist 1994; Wardle 1998). There are several reasons for this, of which perhaps the most important is that the flow time through these shocks is long enough for radiation from molecules to maintain the gas at a low temperature even for shock speeds as high as 50 km s^{-1} . Indeed, Wardle (1998) points out that this process is so effective that such shocks are responsible for much of the infrared H_2 and CO line emission in molecular clouds (Draine & Roberge 1982; Chernoff, McKee & Hollerbach 1982; Smith & Brand 1990; Smith, Brand & Moorhouse 1991; Chrysostomou et al. 1997). The heating due to the currents also raises the temperature of the molecular gas to the point where a number of important chemical reactions proceed at a significant rate (Draine, Roberge & Dalgarno 1983; Flower, Pineau des Forêts & Hartquist 1985; Pineau des

Forêts, Flower Hartquist & Dalgarno 1986; Draine & Katz 1986a,b; Kaufman & Neufeld 1996a,b).

Although the obvious way to determine the steady shock structures is to solve the steady equations directly, this is not a simple matter in the general case. There is no great difficulty when the steady solution can be obtained by integrating through the structure in the appropriate direction (e.g. Wardle & Draine 1987) and one can also deal with solutions containing sub-shocks if the system reduces to two differential equations (Chernoff 1987). However, these are all special cases and the general case of oblique shocks with cooling and chemical reactions is a two point boundary value problem that can only be solved by a relaxation method such as that used by Draine (1980). In that case it is much simpler to use a time dependent code to obtain the steady solution. This also has the advantage that it can be used for unsteady problems in which these effects are important.

A number of numerical schemes for the time dependent equations have been devised (Tóth 1994; Smith & Mac Low 1997; Mac Low & Smith 1997; Stone 1997; Chieze, Pineau de Forêts & Flower 1998; Ciolek & Roberge 2002), but, with the exception of Ciolek & Roberge (2002), these all assume that all the charged particles have a large Hall parameter and are therefore tied to the magnetic field. The system can then be modeled as three fluids: a neutral fluid, an ion fluid and an electron fluid. The ions and electrons may have different temperatures, but the magnetic field forces them to have the same velocity, which can, however, be different from that of the neutral fluid.

In molecular clouds, the assumption that the Hall pa-

arXiv:astro-ph/0308396v1 22 Aug 2003

parameter is large is valid for electrons, ions and small grains such as polycyclic aromatic hydrocarbons (PAH), but not for grains whose radius, a_g , is larger than about 10^{-5} cm. Pilipp & Hartquist (1994) and Wardle (1998) have shown that a significant charge density of particles for which the Hall parameter is $O(1)$ has a profound effect on the shock structures. In particular, such particles induce a Hall resistivity which can lead to substantial rotation of the transverse field within the shock structure. For this reason, Ciolek & Roberge (2002) devised an algorithm for time dependent equations that include a significant charge density of particles whose Hall parameter is not large enough for them to be tied to the field. However, as we shall see, the stable timestep for their algorithm can become very small, especially if there is a significant Hall resistivity. This paper describes an algorithm that does not suffer from this restriction.

Although the emphasis here is on shocks in molecular clouds, the algorithm is quite general and is efficient for any problem in which either ambi-polar diffusion or the Hall effect, or both are important. In particular, although ambi-polar diffusion in molecular clouds is due to drift between neutrals and charged particles, it can also arise due to drift between electrons and ions in plasmas with a small fraction of neutrals if the density is high enough for the ion Hall parameter to be $O(1)$ (e.g. Sano & Stone 2002).

2 MULTI-FLUID EQUATIONS

Consider a set of N fluids for which the generic one dimensional equations are ($i = 1 \dots N$)

$$\frac{\partial \rho_i}{\partial t} + \frac{\partial \rho_i u_i}{\partial x} = \sum_{j \neq i}^N s_{ij}, \quad (1)$$

$$\begin{aligned} \frac{\partial \rho_i \mathbf{q}_i}{\partial t} + \frac{\partial}{\partial x} (\rho_i u_i \mathbf{q}_i + p_i \hat{\mathbf{i}}) &= \alpha_i \rho_i (\mathbf{E} + \mathbf{q}_i \wedge \mathbf{B}) \\ &+ \sum_{j \neq i}^N \mathbf{f}_{ij}, \end{aligned} \quad (2)$$

$$\begin{aligned} \frac{\partial e_i}{\partial t} + \frac{\partial}{\partial x} [u_i (e_i + p_i + \frac{1}{2} \rho_i q_i^2)] &= H_i + \sum_{j \neq i}^N G_{ij} \\ &+ \alpha_i \rho_i \mathbf{q}_i \cdot (\mathbf{E} + \mathbf{q}_i \wedge \mathbf{B}). \end{aligned} \quad (3)$$

Here $\mathbf{q}_i = (u_i, v_i, w_i)$ are the velocities, α_i the charge to mass ratios, e_i the total energies and $\hat{\mathbf{i}}$ the unit vector in the x direction. We have

$$e_i = \rho_i (U_i + \frac{1}{2} \mathbf{q}_i^2)$$

where U_i is the internal energy per unit mass of fluid i . We shall assume that

$$U_i = W_i + \frac{p_i}{\rho_i (\gamma_i - 1)}$$

where W_i is the energy associated with the internal states of the particles of fluid i . It can include ionization energy, chemical binding energy etc.

The source terms are: s_{ij} – mass transfer rate from fluid j to fluid i ; \mathbf{f}_{ij} – momentum transfer rate from fluid j to fluid i ; G_{ij} – energy transfer rate from fluid j to fluid i ; H_i – external energy source/sink for fluid i . Global mass, energy

and momentum conservation clearly require that $s_{ij} = -s_{ji}$, $\mathbf{f}_{ij} = -\mathbf{f}_{ji}$ and $G_{ij} = -G_{ji}$. Draine (1986) derives expressions for these terms, but for our purpose it is sufficient to consider their general form.

The momentum transfer rate, \mathbf{f}_{ij} , is

$$\mathbf{f}_{ij} = \mathbf{C}_{ij} + s_{ij} \mathbf{q}_j - s_{ji} \mathbf{q}_i,$$

where \mathbf{C}_{ij} describes collisions between the particles of fluids i and j . Since it involves binary collisions and tends to equalise the velocities of the two fluids, it must be of the form

$$\mathbf{C}_{ij} = \rho_i \rho_j K_{ij}(T_i, T_j, |\mathbf{q}_j - \mathbf{q}_i|) (\mathbf{q}_j - \mathbf{q}_i),$$

where T_i and T_j are the temperatures of fluids i and j . Since global momentum conservation requires $\mathbf{C}_{ij} = -\mathbf{C}_{ji}$, we must have $\mathbf{K}_{ij} = \mathbf{K}_{ji}$.

The energy transfer rate, G_{ij} , is

$$G_{ij} = \mathbf{q}_i \cdot \mathbf{C}_{ij} + s_{ij} e_j - s_{ji} e_i + D_{ij},$$

where D_{ij} describes the effect of collisions between the particles of fluids i and j . Like \mathbf{C}_{ij} , it involves binary collisions and tends to produce equilibrium between the two fluids. It must therefore be of the form

$$D_{ij} = \rho_i \rho_j L_{ij}(T_i, T_j, |\mathbf{q}_j - \mathbf{q}_i|).$$

with $L_{ij} = 0$ when $T_i = T_j$ and $\mathbf{q}_i = \mathbf{q}_j$. Global energy conservation requires

$$G_{ij} = \mathbf{q}_i \cdot \mathbf{C}_{ij} + D_{ij} = -G_{ji} = -\mathbf{q}_j \cdot \mathbf{C}_{ij} + D_{ji}.$$

The fields are determined from Maxwell's equations, which reduce to

$$\frac{\partial B_x}{\partial t} = 0, \quad \frac{\partial B_y}{\partial t} = \frac{\partial E_z}{\partial x}, \quad \frac{\partial B_z}{\partial t} = -\frac{\partial E_y}{\partial x}, \quad (4)$$

$$\frac{\partial B_y}{\partial x} = J_z, \quad \frac{\partial B_z}{\partial x} = -J_y \quad (5)$$

since the displacement current may be neglected. The current, \mathbf{J} , is given by

$$\mathbf{J} = \sum_{i=1}^N \alpha_i \rho_i \mathbf{q}_i. \quad (6)$$

and we also have charge neutrality

$$\sum_{i=1}^N \alpha_i \rho_i = 0. \quad (7)$$

The units for \mathbf{E} , \mathbf{B} and \mathbf{J} are such that the speed of light and the factor 4π do not appear.

The above equations are extremely general and include those that other authors have used to model shocks in molecular clouds as special cases. Despite this generality, they do assume that each fluid can be described by the hydrodynamic approximation, which is only true if the interactions between particles of the different fluids are much weaker than those between particles of the same fluid.

In the usual applications, the mass is dominated by a fluid, $i = 1$ say, consisting of neutral particles, which obviously has zero charge to mass ratio. The other fluids are: an electron fluid, $i = 2$; an ion fluid, $i = 3$; fluids consisting of grains of various types and sizes, $i = 4 \dots N$. The validity of the hydrodynamic approximation for systems consisting

only of neutrals, electrons and ions has been discussed by Draine (1986) and Chernoff (1987). They conclude that the hydrodynamic approximation is valid for the neutrals and electrons, both of which should have a Maxwellian distribution, but this may not be true for the ions.

The grain fluids are obviously very different since they consist of particles with much larger masses than the other fluids. Their thermal velocity dispersion is therefore small compared to the drift velocities, which means that all the particles of a particular size and type have the same velocity. The hydrodynamic approximation with zero pressure is therefore appropriate for the grain fluids.

Although it is possible to construct a numerical scheme for these equations as they stand, this would not be suitable for the conditions in shocks in molecular clouds. Consider the neutral momentum equation and suppose that the drift velocities are small compared to the thermal velocity dispersion of the neutrals, as they must be near the upstream or downstream ends of the shock structure. The collision term is then approximately

$$\sum_{i=2}^N \mathbf{C}_{1i} = \sum_{i=2}^N \rho_1 \rho_i K_{1i}(T_1, T_i, 0) (\mathbf{q}_i - \mathbf{q}_1).$$

If q_c is a typical velocity, such as the shock velocity relative to the upstream fluid, then a balance between this term and the inertia terms induces a length scale

$$l_{c1} = \frac{q_c}{\sum_{i=2}^N K_{1i}(T_1, T_i, 0) \rho_i}.$$

It is clear that l_{c1} determines the shock thickness. Then since $\rho_i \ll \rho_1$ for all $i > 1$, the equivalent length scales for the other fluids are

$$l_{ci} = \frac{q_c}{K_{1i}(T_1, T_j, 0) \rho_1},$$

which means that $l_{ci} \ll l_{c1}$.

The charged fluids are also acted on by electromagnetic forces, which induce a length scale

$$l_{ei} = \frac{q_c}{\alpha_i B},$$

which is the Larmor radius of particles with velocity q_c .

Provided either $l_{ci} \ll l_{c1}$ or $l_{ei} \ll l_{c1}$, the inertia and pressure terms can be ignored in the momentum equation for fluid i . Since this is generally true, the momentum equations for all fluids except the neutral fluid reduce to

$$\alpha_i \rho_i (\mathbf{E} + \frac{\mathbf{q}_i}{c} \wedge \mathbf{B}) + \mathbf{f}_{i1} = 0, \quad (8)$$

where the fact that $\rho_i \ll \rho_1$ for all i has allowed us to ignore momentum transfer from all but the neutral fluid. The same arguments tell us that in this case the energy equations for the charged fluids reduce to

$$H_i + G_{i1} + \alpha_i \rho_i \mathbf{q}_i \cdot (\mathbf{E} + \mathbf{q}_i \wedge \mathbf{B}) = 0 \quad (9)$$

If $l_{ei} \ll l_{c1}$, then particles i are closely tied to the field lines. It is convenient to define a Hall parameter, β_i , for each charged fluid by

$$\beta_i = \frac{l_{ci}}{l_{ei}} = \frac{\alpha_i B}{K_{1i} \rho_1}.$$

The ions and electrons have $\beta_i \gg 1$ and are therefore tied to the field, whereas the grains are not since they typically have $\beta_i \simeq 1$.

3 NUMERICAL METHOD

Our method deals with the same equations as Ciolek & Roberge (2002), but uses a somewhat different approach, which, as we shall see, leads to a more robust and efficient scheme.

3.1 Equations for the Neutral Fluid

Since $\mathbf{f}_{ij} = -\mathbf{f}_{ji}$, the reduced momentum equations for the charged fluids, (8), the charge neutrality condition, (7) and the expression for the current, (6) give

$$\sum_{i=2}^N \mathbf{f}_{1i} = - \sum_{i=2}^N \mathbf{f}_{i1} = \sum_{i=2}^N \alpha_i \rho_i (\mathbf{E} + \mathbf{q}_i \wedge \mathbf{B}) = \mathbf{J} \wedge \mathbf{B}.$$

The momentum equation for the neutral fluid, (2), then becomes

$$\frac{\partial \rho_1 \mathbf{q}_1}{\partial t} + \frac{\partial}{\partial x} (\rho_1 u_1 \mathbf{q}_1 + p_1 \hat{\mathbf{i}}) = \sum_{i=2}^N \mathbf{f}_{1i} = \mathbf{J} \wedge \mathbf{B}. \quad (10)$$

Similarly, the reduced energy equations, (9), give

$$\begin{aligned} \sum_{i=2}^N G_{1i} &= - \sum_{i=2}^N G_{i1} = \sum_{i=2}^N [H_i + \alpha_i \rho_i \mathbf{q}_i \cdot (\mathbf{E} + \mathbf{q}_i \wedge \mathbf{B})] \\ &= \mathbf{J} \cdot \mathbf{E} + \sum_{i=2}^N [H_i + \alpha_i \rho_i \mathbf{q}_i \cdot (\mathbf{q}_i \wedge \mathbf{B})]. \end{aligned}$$

The energy equation for the neutrals, (3), then becomes

$$\begin{aligned} \frac{\partial e_1}{\partial t} + \frac{\partial}{\partial x} [u_1 (e_1 + p_1 + \frac{1}{2} \rho_1 q_1^2)] &= H_1 + \sum_{i=2}^N G_{1i} \\ &= \mathbf{J} \cdot \mathbf{E} + \sum_{i=1}^N [H_i + \alpha_i \rho_i \mathbf{q}_i \cdot (\mathbf{q}_i \wedge \mathbf{B})]. \end{aligned} \quad (11)$$

Equations (10), (11) and the continuity equation for the neutrals, (1) with $i = 1$, are just the ordinary gas dynamic equations with source terms. They can be written in the form

$$\frac{\partial \mathbf{Q}}{\partial t} + \frac{\partial \mathbf{F}}{\partial x} = \mathbf{S}, \quad (12)$$

where

$$\mathbf{Q} = (\rho_1, \rho_1 \mathbf{q}_1, e_1),$$

is a vector of conserved variables, \mathbf{F} is the vector of fluxes and \mathbf{S} is the vector of source terms. We have $\mathbf{F} = \mathbf{F}(\mathbf{Q})$, but the source term depends upon the magnetic field and the state of the other fluids. We therefore write

$$\mathbf{S} = \mathbf{S}(\mathbf{Q}, \mathbf{V})$$

where \mathbf{V} is a vector representing \mathbf{B} , ρ_i , \mathbf{q}_i etc.

3.2 Numerical Scheme for the Neutral Fluid

Equations (12) are solved using the second order Godunov scheme described in Falle (1991). This is a conservative scheme in which the numerical solution at time t_n in the cell with $(j - 1/2)\Delta x \leq x \leq (j + 1/2)\Delta x$ is defined to be the volume average

$$\mathbf{Q}_j^n = \frac{1}{\Delta x} \int_{(j-1/2)\Delta x}^{(j+1/2)\Delta x} \mathbf{U}(t_n, x) dx.$$

Integrating (12) over the j th cell and from t_n to $t_{n+1} = t_n + \Delta t_n$, gives

$$\begin{aligned} \frac{1}{\Delta t_n} (\mathbf{Q}_j^{n+1} - \mathbf{Q}_j^n) + \frac{1}{\Delta x} (\mathbf{F}_{j+1/2}^{n+1/2} - \mathbf{F}_{j-1/2}^{n+1/2}) \\ = \mathbf{S}_j^{n+1/2}, \end{aligned} \quad (13)$$

where $\mathbf{F}_{j\pm 1/2}^{n+1/2}$ are the time averages of the fluxes at the cell edges and $\mathbf{S}_j^{n+1/2}$ is the time average of the integral of the source term over the cell.

We start by using equation (13) to compute a first order approximation, $\mathbf{Q}_j^{n+1/2}$, to the solution at the half time, $t_{n+1/2} = t_n + \Delta t_n/2$. In this step the fluxes and source term are approximated by

$$\mathbf{F}_{j+1/2}^{n+1/2} = \mathbf{F}_*(\mathbf{Q}_j^n, \mathbf{Q}_{j+1}^n), \quad \mathbf{S}_j^{n+1/2} = \mathbf{S}(\mathbf{Q}_j^n, \mathbf{V}_j^n),$$

where $\mathbf{F}_*(\mathbf{Q}_L, \mathbf{Q}_R)$ is the flux in the resolved state for a gas dynamic Riemann problem for which the left and right states are \mathbf{Q}_L and \mathbf{Q}_R .

To make the scheme second order in space, we use the solution at the half time to construct an average gradient of the primitive variables, $\mathbf{P} = (\rho_1, \mathbf{q}_1, p_1)$, in the i th cell

$$\left(\frac{\partial \mathbf{P}}{\partial x} \right)_j^{n+1/2} = \frac{1}{\Delta x} av(\mathbf{P}_{j+1}^{n+1/2} - \mathbf{P}_j^{n+1/2}, \mathbf{P}_j^{n+1/2} - \mathbf{P}_{j-1}^{n+1/2}),$$

where the averaging function is

$$av(a, b) = \begin{cases} 0 & \text{if } ab < 0, \\ \frac{a^2 b + ab^2}{a^2 + b^2} & \text{otherwise.} \end{cases}$$

The averaging function acts as a non-linear switch that reduces the scheme to first order in regions with large second derivatives, such as shocks etc (see e.g. van Leer 1977).

The solution at $t_{n+1} = t_n + \Delta t_n$ is then calculated from (13) with

$$\mathbf{F}_{j+1/2}^{n+1/2} = \mathbf{F}_*[\mathbf{Q}(\mathbf{P}_L), \mathbf{Q}(\mathbf{P}_R)],$$

where

$$\mathbf{P}_L = \mathbf{P}_j^{n+1/2} + \frac{1}{2} \Delta x \left(\frac{\partial \mathbf{P}}{\partial x} \right)_j^{n+1/2}$$

$$\mathbf{P}_R = \mathbf{P}_{j+1}^{n+1/2} - \frac{1}{2} \Delta x \left(\frac{\partial \mathbf{P}}{\partial x} \right)_{j+1}^{n+1/2},$$

and the source term given by

$$\mathbf{S}_j^{n+1/2} = \mathbf{S}(\mathbf{Q}_j^{n+1/2}, \mathbf{V}_j^{n+1/2}).$$

This is obviously not a complete scheme since we have yet to devise a method of advancing the variables, \mathbf{V} , describing the field and charged fluids.

3.3 Equations for the Charged Fluids and Fields

The reduced momentum equations, (8) and the expression for the current, (6) can be solved for the electric field. It is standard practice to write the result in the form

$$\mathbf{E} = -\mathbf{q} \wedge \mathbf{B} + r_0 \frac{(\mathbf{J} \cdot \mathbf{B})\mathbf{B}}{B^2} + r_1 \frac{\mathbf{J} \wedge \mathbf{B}}{B} - r_2 \frac{(\mathbf{J} \wedge \mathbf{B}) \wedge \mathbf{B}}{B^2} \quad (14)$$

(Cowling 1957; Nakano & Umebayashi 1986). Here r_0 is the resistivity along the field, r_1 is the Hall resistivity and r_2 is the ambi-polar resistivity. If we define the conductivity parallel to the field,

$$\sigma_0 = \frac{1}{B} \sum_{i=2}^N \alpha_i \rho_i \beta_i$$

the Hall conductivity,

$$\sigma_1 = \frac{1}{B} \sum_{i=2}^N \frac{\alpha_i \rho_i}{(1 + \beta_i^2)}$$

and the Pedersen conductivity,

$$\sigma_2 = \frac{1}{B} \sum_{i=2}^N \frac{\alpha_i \rho_i \beta_i}{(1 + \beta_i^2)}$$

then the resistivities are

$$r_0 = 1/\sigma_0, \quad r_1 = \sigma_1/(\sigma_1^2 + \sigma_2^2), \quad r_2 = \sigma_2/(\sigma_1^2 + \sigma_2^2)$$

Substituting (14) into the Faraday equations (4) and using Ampere's law (5) to eliminate \mathbf{J} gives the induction equation

$$\frac{\partial \mathbf{B}}{\partial t} + \frac{\partial \mathbf{M}}{\partial x} = \frac{\partial}{\partial x} \mathbf{R} \frac{\partial \mathbf{B}}{\partial x}, \quad (15)$$

where the hyperbolic flux is

$$\mathbf{M} = (0, uB_y - vB_x, uB_z - wB_x),$$

and the resistance matrix is

$$\mathbf{R} = r_0 \mathbf{R}_0 + r_1 \mathbf{R}_1 + r_2 \mathbf{R}_2,$$

with

$$\mathbf{R}_0 = \begin{pmatrix} \frac{B_z^2}{B^2} & -\frac{B_y B_z}{B^2} \\ -\frac{B_y B_z}{B^2} & \frac{B_y^2}{B^2} \end{pmatrix},$$

$$\mathbf{R}_1 = \begin{pmatrix} 0 & \frac{B_x}{B} \\ -\frac{B_x}{B} & 0 \end{pmatrix},$$

$$\mathbf{R}_2 = \begin{pmatrix} 1 - \frac{B_z^2}{B^2} & \frac{B_y B_z}{B^2} \\ \frac{B_y B_z}{B^2} & 1 - \frac{B_y^2}{B^2} \end{pmatrix}.$$

Equation (15) can be used to advance the field, but, as we shall see, an explicit approximation to this is very inefficient if the Hall term is much larger than the ambi-polar diffusion term.

3.4 Numerical Stability

The presence of the diffusive terms on the right hand side of equation (15) has some important implications for any numerical scheme, the most obvious of which is that the stable time step for any explicit scheme will be proportional to the square of the mesh spacing. What is less obvious is

that the Hall term places an even more severe restriction on the stable time step for explicit schemes.

In order to see this, suppose that the diffusive flux in equation (15) is much larger than the hyperbolic flux. Since r_0 is much smaller than the other resistivities provided that there is a significant charge density of particles with large β , we can also ignore the term $r_0 \mathbf{R}_0$ in the resistance matrix.

If we now linearise (15) about a state in which $B_z = 0$ and the field makes an angle θ with the x-axis, then

$$\mathbf{R} = \begin{pmatrix} r_2 & r_1 \cos \theta \\ -r_1 \cos \theta & r_2 \cos^2 \theta \end{pmatrix}.$$

Now let \mathbf{B}_j^n be a numerical approximation to $\mathbf{B}(t_n, j\Delta x)$ and consider the obvious scheme

$$\begin{aligned} \frac{1}{\Delta t}(\mathbf{B}_j^{n+1} - \mathbf{B}_j^n) = \\ \frac{1}{\Delta x^2} \mathbf{R}[(1 - \mu)(\mathbf{B}_{j+1}^n - 2\mathbf{B}_j^n + \mathbf{B}_{j-1}^n) \\ + \mu(\mathbf{B}_{j+1}^{n+1} - 2\mathbf{B}_j^{n+1} + \mathbf{B}_{j-1}^{n+1})], \end{aligned} \quad (16)$$

where $0 \leq \mu \leq 1$. This scheme is purely explicit for $\mu = 0$, purely implicit for $\mu = 1$ and time centred (Crank-Nicolson) for $\mu = 1/2$. For a numerical wave of the form

$$\mathbf{B}_j^n = \mathbf{B}^n \exp(i\omega j),$$

we get

$$\mathbf{B}^{n+1} = \mathbf{A} \mathbf{B}^n,$$

where the amplification matrix, \mathbf{A} is

$$\mathbf{A} = [\mathbf{I} + \nu \mu \mathbf{R}]^{-1} [\mathbf{I} - \nu(1 - \mu)\mathbf{R}],$$

with

$$\nu = \frac{2\Delta t(1 - \cos \omega)}{\Delta x^2},$$

and \mathbf{I} the 2×2 identity matrix. Clearly the most restrictive condition on the timestep is for the ± 1 mode, $\cos \omega = -1$, for which

$$\nu = \frac{4\Delta t}{\Delta x^2}. \quad (17)$$

3.4.1 Explicit Scheme ($\mu = 0$)

In this case the eigenvalues of \mathbf{A} are given by

$$\begin{aligned} \lambda^2 + (\nu r_2 \cos^2 \theta - 2 + \nu r_2) \lambda \\ + 1 - \nu r_2 \cos^2 \theta - \nu r_2 + \nu^2 r_1^2 \cos^2 \theta + \nu^2 r_2^2 \cos^2 \theta = 0. \end{aligned}$$

This has real roots if

$$r_1 \cos \theta \leq \frac{1}{2} r_2 \sin^2 \theta,$$

in which case stability requires

$$\nu \leq \frac{4}{[r_2 \cos^2 \theta + r_2 + \sqrt{(r_2^2 \sin^4 \theta - 4r_1^2 \cos^2 \theta)]}.$$

This increases with $r_1 \cos \theta$, so that the Hall term increases the stable time step, but when the eigenvalues of \mathbf{A} become complex, the stability condition is

$$\nu \leq \frac{r_2(1 + \cos^2 \theta)}{(r_1^2 + r_2^2) \cos^2 \theta}.$$

This tells us that the stable time step tends to zero as the Hall term becomes large compared to ambi-polar diffusion, which means that an explicit scheme is very inefficient in such cases. This would seem to be the explanation for the severe restrictions on the stable timestep experienced by Hollerbach & Rüdiger (2002) in their calculations of the Hall effect in neutron stars.

3.4.2 Crank-Nicolson Scheme ($\mu = 1/2$)

The eigenvalues of \mathbf{A} are now given by

$$\begin{aligned} (2\nu r_2 \cos^2 \theta + 2\nu r_2 + 4 + \nu^2 r_1^2 \cos^2 \theta + \nu^2 r_2^2 \cos^2 \theta) \lambda^2 \\ + (2\nu^2 r_1^2 \cos^2 \theta + 2\nu^2 r_2^2 \cos^2 \theta - 8) \lambda \\ + 4 + \nu^2 r_1^2 \cos^2 \theta - 2\nu r_2 \cos^2 \theta - 2\nu r_2 + \nu^2 r_2^2 \cos^2 \theta = 0, \end{aligned}$$

whose roots are

$$\lambda = \frac{4 - \nu^2 \cos^2 \theta (r_1^2 + r_2^2) \pm 2\nu \sqrt{(r_2^2 \sin^4 \theta - 4r_1^2 \cos^2 \theta)}}{4 + 2\nu r_2(1 + \cos^2 \theta) + \nu^2 \cos^2 \theta (r_1^2 + r_2^2)}.$$

As we would expect, $|\lambda| \leq 1$ for all ν , so the scheme is unconditionally stable.

One might wonder whether there is some other explicit scheme with better stability properties. That this is unlikely can be seen by looking at the nature of the equation when the Hall term is dominant. We then get a dispersive wave equation for whistler waves with

$$\omega^2 = \frac{r_1^2 B_x^2}{B^2} k^4,$$

so that both the phase and group velocities tend to infinity as the wavenumber tends to infinity. This not only explains why the first order explicit approximation, (16), to the Hall term is unstable, but also suggests that there is no stable explicit approximation. For example, the second order explicit scheme described by Sano & Stone (2002) is unconditionally unstable when the Hall term is dominant, although this was not apparent in their test calculation because the numerical resolution was low enough for the scheme to be stabilized by the hyperbolic term.

Ciolek & Roberge (2002) do not use (15) to advance the field, instead they write \mathbf{E} in terms of the velocity, \mathbf{q}_3 of the ions

$$\mathbf{E} = -\mathbf{q}_3 \wedge \mathbf{B},$$

which is valid since $\beta_3 \gg 1$. They then use the Faraday equation, (4), to obtain an evolution equation for \mathbf{B} . This has the disadvantage that, since there is no simple way of making such a scheme implicit, it requires a very small time step at high resolution, particularly when the Hall term is large compared to ambi-polar diffusion.

3.5 Numerical Scheme for the Charged Fluids and Fields

In order to obtain the state of the charged fluids and fields, $\mathbf{V}_{n+1/2j}$ at the half time, we first advance the magnetic field with the first order scheme

$$\begin{aligned} \frac{1}{\Delta t}(\mathbf{B}_j^{n+1/2} - \mathbf{B}_j^n) + \frac{1}{\Delta x}(\mathbf{M}_{j+1/2}^n - \mathbf{M}_{j-1/2}^n) = \\ \frac{1}{\Delta x^2} \mathbf{R}_j^n (\mathbf{B}_{j+1}^{n+1/2} - 2\mathbf{B}_j^{n+1/2} + \mathbf{B}_{j-1}^{n+1/2}), \end{aligned} \quad (18)$$

where $\mathbf{R}_j^n = \mathbf{R}(\mathbf{V}_j^n)$. Note that the term on the right hand side are calculated implicitly, whereas the hyperbolic term is calculated explicitly. This is a block tridiagonal equation for $\mathbf{B}^{n+1/2}$ with the blocks consisting of 2×2 matrices and can readily be solved by Gaussian elimination.

It would be nice to use a Riemann problem to compute the hyperbolic flux, \mathbf{M} , but this is not possible because we would have to solve a Riemann problem in which the magnetic field does not exert a force on the gas. In general the solution to such problems contains discontinuities in the tangential velocities which are incompatible with the induction equation. We therefore have to be content with a centred approximation to the hyperbolic flux

$$\overline{\mathbf{M}}_{j+1/2}^n = \frac{1}{2}(\mathbf{M}_{j+1}^n + \mathbf{M}_j^n).$$

This is perfectly satisfactory as long as the resistive terms and numerical resolution are such as that the magnetic field appears continuous on the grid.

The densities of the charged fluids can be calculated from an explicit upwind approximation to the continuity equations and the current from a centred approximation to the Ampere's law, (5), using the field at the half time. Given \mathbf{J} , \mathbf{B} and the state of the neutral fluid at the half time, we can calculate $\mathbf{V}_j^{n+1/2}$ from the reduced momentum equations, (8), the expression for the current, (6), and the reduced energy equations, (9). Note that these equations have to be solved by iteration if the interaction coefficients, K_{1i} , depend upon the velocities, but since the solution at the old time provides a very good initial guess, this is not expensive.

$\mathbf{V}_j^{n+1/2}$ can then be used to calculate the source term at the half time so that the neutral solution can be advanced to the full time using (13) with the second order fluxes. The densities of the charged fluids can also be advanced using $\mathbf{V}_j^{n+1/2}$ in a second order approximation to their continuity equations. As we shall see, this algorithm is well behaved even when some of the charged species have very large Hall parameters.

The magnetic field is advanced explicitly to the full time using fluxes computed from the solution at the half time

$$\frac{1}{\Delta t}(\mathbf{B}_j^{n+1} - \mathbf{B}_j^n) + \frac{1}{\Delta x}(\mathbf{M}_{j+1/2}^{n+1/2} - \mathbf{M}_{j-1/2}^{n+1/2}) = \frac{1}{\Delta x^2} \mathbf{R}_j^{n+1/2} (\mathbf{B}_{j+1}^{n+1/2} - 2\mathbf{B}_j^{n+1/2} + \mathbf{B}_{j-1}^{n+1/2}).$$

Although this is explicit, the fact that the field at the half time has been calculated implicitly ensures the same stability properties as a Crank-Nicolson. Finally the neutral solution, charged fluid densities and magnetic field can be used to calculate the charged fluid velocities and temperatures at the full time in the same way as for $\mathbf{V}_j^{n+1/2}$.

4 TEST CALCULATIONS

In order to test the code described in the previous section, we compare the results for steady shocks with those obtained by a direct solution of the steady equations. The numerical solution was obtained by imposing the upstream and downstream states at the right and left boundaries of the domain with a discontinuity in the middle of the domain and then integrating until the steady state is reached.

4.1 Steady Solutions

In order to calculate the steady solution, we start by transforming the induction equation, (15), to a frame in which the shock is steady and then setting the time derivative to zero. This gives

$$\frac{d\mathbf{M}}{dx} = \frac{d}{dx} \mathbf{R} \frac{d\mathbf{B}}{dx},$$

which can be integrated to give

$$\mathbf{M} - \mathbf{M}_L = \mathbf{M} - \mathbf{M}_R = \mathbf{R} \frac{d\mathbf{B}}{dx}, \quad (19)$$

where the suffices L , R , denote the upstream and downstream states respectively. The shock relations ensure that $\mathbf{M}_L = \mathbf{M}_R$ so that the upstream and downstream states are fixed points of this equation.

We confine ourselves to the case where the neutral gas is isothermal, so that the steady versions of the neutral equations can be all be integrated to give

$$\begin{aligned} \rho u &= Q, & \rho u^2 + a^2 \rho + \frac{1}{2} B^2 &= P_x \\ \rho u v - B_x B_y &= P_y, & \rho u w - B_x B_z &= P_z \end{aligned}$$

where Q , P_x , P_y and P_z are constants and a is the isothermal neutral sound speed. Here we have used Ampere's law, (5), to write \mathbf{J} in terms of \mathbf{B} in the momentum equation. These equations can be solved to give ρ and $\mathbf{q} = (u, v, w)$ as functions of \mathbf{B} .

The charged fluid densities are given by

$$\rho_i u_i = Q_i, \quad (20)$$

where the Q_i are constants. The reduced momentum equations for the charged fluids, (8), give us $3N - 3$ equations for the $3N - 3$ components of the charged fluid velocities and the 3 components of the electric field. In the steady case, the Faraday equation, (4), tells us that E_y and E_z are constant and equal to their values in the upstream state, so that only E_x is unknown. We therefore have $3N - 2$ unknowns and $3N - 3$ equations. The remaining equation can be obtained from (20) and the charge neutrality condition, (7).

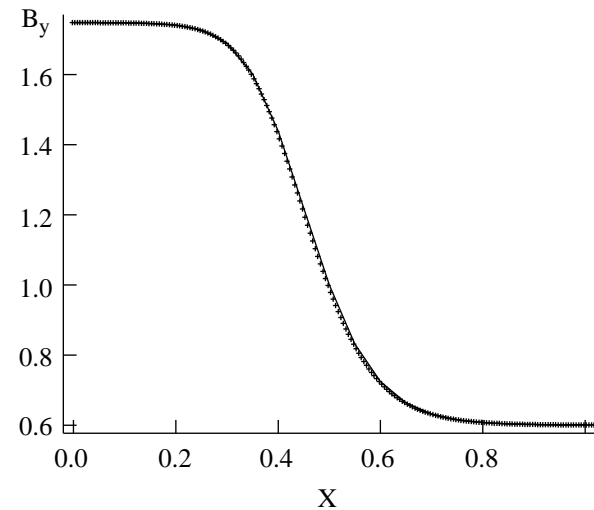
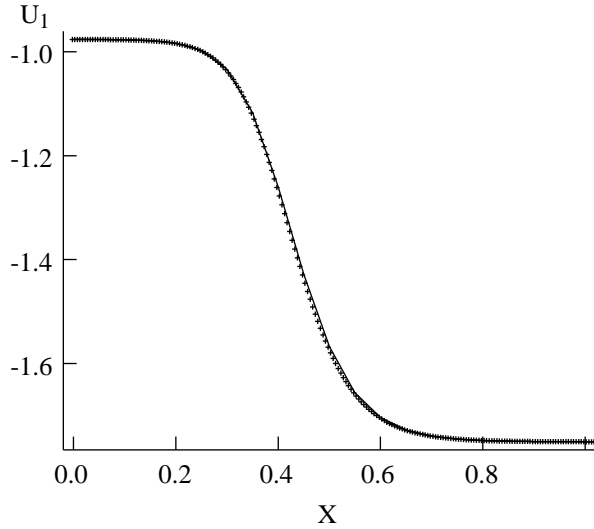
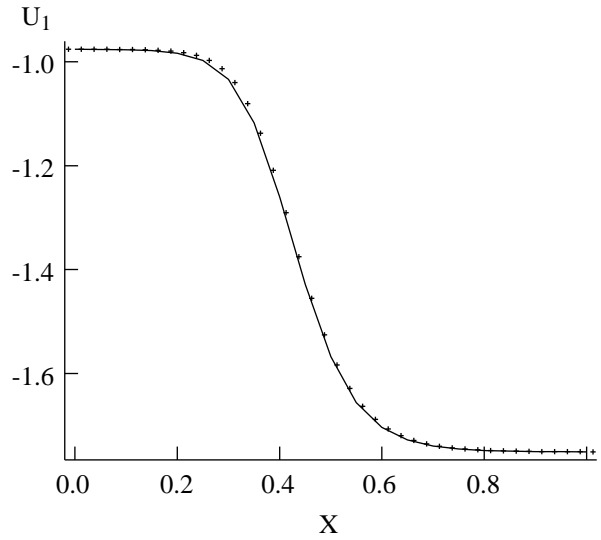
Given \mathbf{B} , we can therefore calculate the neutral velocities and the charged densities and hence \mathbf{M} and the resistance matrix, \mathbf{R} . We shall confine ourselves to cases for which the downstream state is a saddle point and the upstream state is a sink, in which case the steady solution can be obtained by integrating (19) from downstream to upstream. Since the gas is isothermal, any sub-shock must be at the downstream end of the structure. It is therefore a simple matter to insert a subshock and then to integrate from its upstream side towards the upstream state (see case C).

4.2 Case A (Negligible Hall Effect)

This has two charged fluids, both of which have $\beta \gg 1$, so that the Hall resistivity is negligible. The parameters are given in table 1. This corresponds to an oblique fast shock with an upstream Mach number relative to the fast speed $M_f = 1.5$ and a very small neutral pressure. The charge to mass ratios, α_i , and collision coefficients, $K_{1,i}$ are such that $\beta_2 = -5.831 \cdot 10^6$, $\beta_3 = -5.831 \cdot 10^3$ in the upstream state, which is appropriate for electrons and ions in material with $n_H = 10^6$ and $B = 10^{-3}$ G (Wardle 1998). This gives

Table 1. Parameters for the Test Calculations

Case A					
Upstream	$\rho = 1$	$\mathbf{q} = (-1.7510, 0, 0)$	$\mathbf{B} = (1, 0.6, 0)$	$\rho_2 = 5 \cdot 10^{-8}$	$\rho_3 = 10^{-3}$
Downstream	$\rho = 1.7942$	$\mathbf{q} = (-0.9759, -0.6561, 0)$	$\mathbf{B} = (1, 1.74885, 0)$	$\rho_2 = 8.9712 \cdot 10^{-8}$	$\rho_3 = 1.7942 \cdot 10^{-3}$
	$\alpha_2 = -2 \cdot 10^{12}$	$\alpha_3 = 10^8$	$K_{12} = 4 \cdot 10^5$	$K_{13} = 2 \cdot 10^4$	$a = 0.1$
Case B					
Upstream	as for case A				
Downstream	as for case A				
	$\alpha_2 = -2 \cdot 10^9$	$\alpha_3 = 10^5$	$K_{12} = 4 \cdot 10^2$	$K_{13} = 5 \cdot 10^5$	$a = 0.1$
Case C					
Upstream	$\rho = 1$	$\mathbf{q} = (-6.7202, 0, 0)$	$\mathbf{B} = (1, 0.6, 0)$	$\rho_2 = 5 \cdot 10^{-8}$	$\rho_3 = 10^{-3}$
Downstream	$\rho = 10.421$	$\mathbf{q} = (-0.6449, -1.0934, 0)$	$\mathbf{B} = (1, 7.9481, 0)$	$\rho_2 = 5.2104 \cdot 10^{-7}$	$\rho_3 = 1.0421 \cdot 10^{-2}$
	$\alpha_2 = -2 \cdot 10^{12}$	$\alpha_3 = 10^8$	$K_{12} = 4 \cdot 10^5$	$K_{13} = 2 \cdot 10^4$	$a = 1$


Figure 1. Neutral x velocity and y component of magnetic field for case A with $\Delta x = 5 \cdot 10^{-3}$. The line is the solution to the steady equations and the markers are the time dependent numerical solution.

Figure 2. Neutral x velocity for case A with $\Delta x = 2.5 \cdot 10^{-2}$. The line is the solution to the steady equations and the markers are the time dependent numerical solution.

$r_0 = 2 \cdot 10^{-12}$, $r_1 = 1.16 \cdot 10^{-5}$ and $r_2 = 0.068$, so that the Hall term is negligible compared with ambi-polar diffusion.

From Fig 1, which shows the neutral x velocity and the y component of the magnetic field, it is clear that the agreement between the two solutions is excellent at high resolution. Even at the much lower resolution shown in Fig 2, the errors are very small.

In order to make this quantitative, we define the L_1 error in a primitive variable, P , by

$$\epsilon_P = \frac{1}{(j_1 - j_0)} \sum_{j=j_0}^{j_1} [P_j - P_s(j\Delta x)], \quad (21)$$

where P_j is the numerical solution in cell j and $P_s(x)$ is the solution calculated from the steady equations. Here j_0 and j_1 are such that the region $x_0 = j_0\Delta x$ to $x_1 = j_1\Delta x$ covers the shock structure, but does not include much of the upstream and downstream uniform regions. Since the numerical shock position depends upon the evolution from the initial data, we impose a shift in x on the steady solution so as to minimize the error.

For case A, with $x_0 = -0.06$, $x_1 = 0.94$, the error in

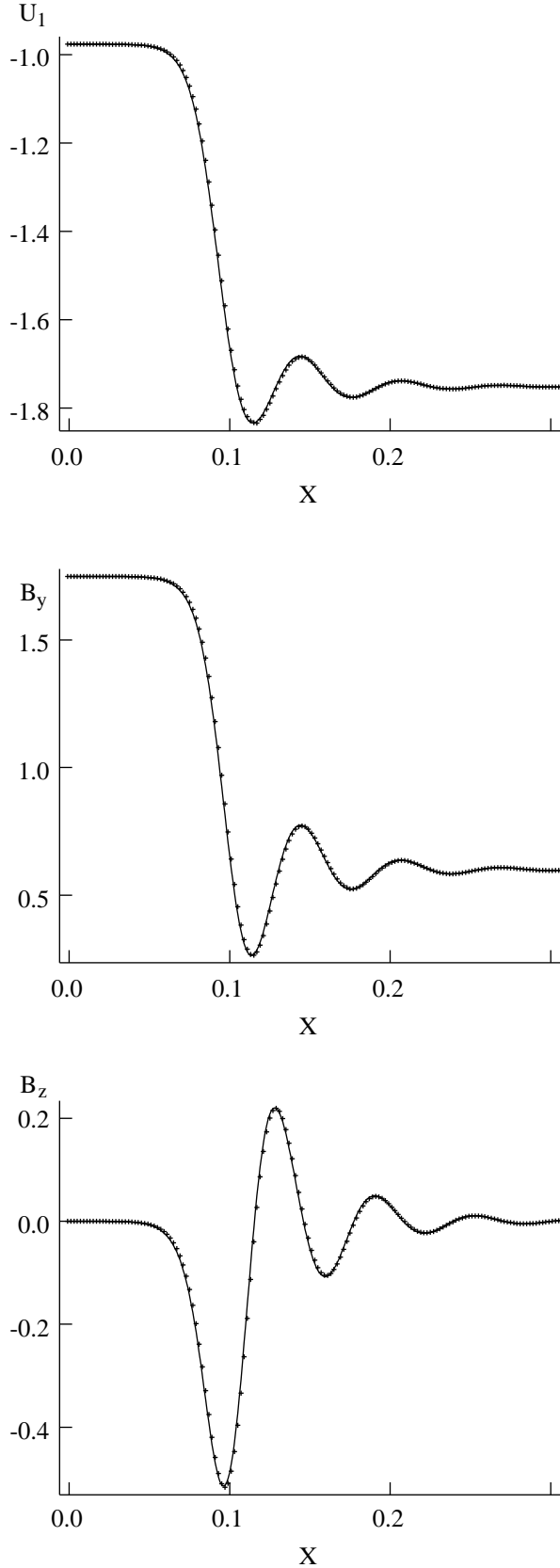


Figure 3. Neutral x velocity and y,z components of magnetic field for case B $\Delta x = 2 \cdot 10^{-3}$. The line is the solution to the steady equations and the markers are the time dependent numerical solution.

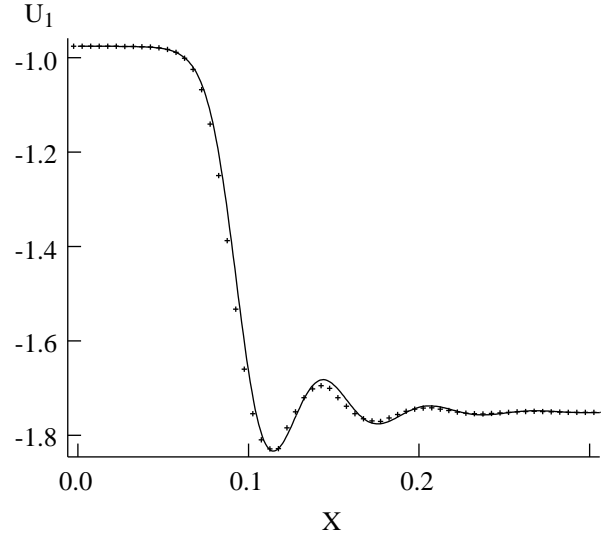


Figure 4. Neutral x velocity for case B with $\Delta x = 5 \cdot 10^{-3}$. The line is the solution to the steady equations and the markers are the time dependent numerical solution.

the neutral x velocity is $\epsilon_{u_1} = 5.68 \cdot 10^{-5}$ for $\Delta x = 0.005$ and $\epsilon_{u_1} = 1.26 \cdot 10^{-3}$ for $\Delta x = 0.025$. This corresponds to $\epsilon_{u_1} \propto \Delta x^{1.92}$, i.e. very nearly second order convergence. For $\Delta x = 0.0125$, the corresponding error is $3.52 \cdot 10^{-4}$, which, when compared to $\Delta x = 0.005$, gives a convergence rate of $\epsilon_{u_1} \propto \Delta x^{1.96}$. This indicates that the asymptotic convergence is indeed second order, as we would expect for a smooth solution.

4.3 Case B (Large Hall Effect)

This case also has two charged fluids with $\beta_2 = -5.831 \cdot 10^6$ as in case A, but with $\beta_3 = 0.2332$. This gives $r_0 = 2 \cdot 10^{-9}$, $r_1 = 0.0116$ and $r_2 = 0.00272$, so that the Hall term dominates the ambi-polar term. In all other respects, the upstream and downstream states are for Case A.

This calculation is more demanding than case A since the fact that the Hall term is dispersive means that the upstream state is now a stable spiral instead of a stable node. The shock structure therefore contains large oscillations whose wavelength is significantly smaller than the total width of the shock structure. Nevertheless, Fig 3 shows that at sufficiently high resolution, the agreement between the solutions is excellent and Fig 4 shows that it is still satisfactory even when there are only ~ 50 mesh points in the shock structure. Note that, as we would expect, there is a significant z component of the magnetic field in this case.

In this case, with $x_0 = 0$, $x_1 = 0.4$, the error in the neutral x velocity is $\epsilon_{u_1} = 3.79 \cdot 10^{-4}$ for $\Delta x = 0.002$ and $\epsilon_{u_1} = 2.37 \cdot 10^{-3}$ for $\Delta x = 0.005$. This gives $\epsilon_{u_1} \propto \Delta x^{2.0}$, which shows that at we have already reached second order convergence rate at these resolutions. Again, this is what we would expect for a smooth solution. Note, however, that since the solution contains more structure than case A, the errors are larger even though the resolution is higher.

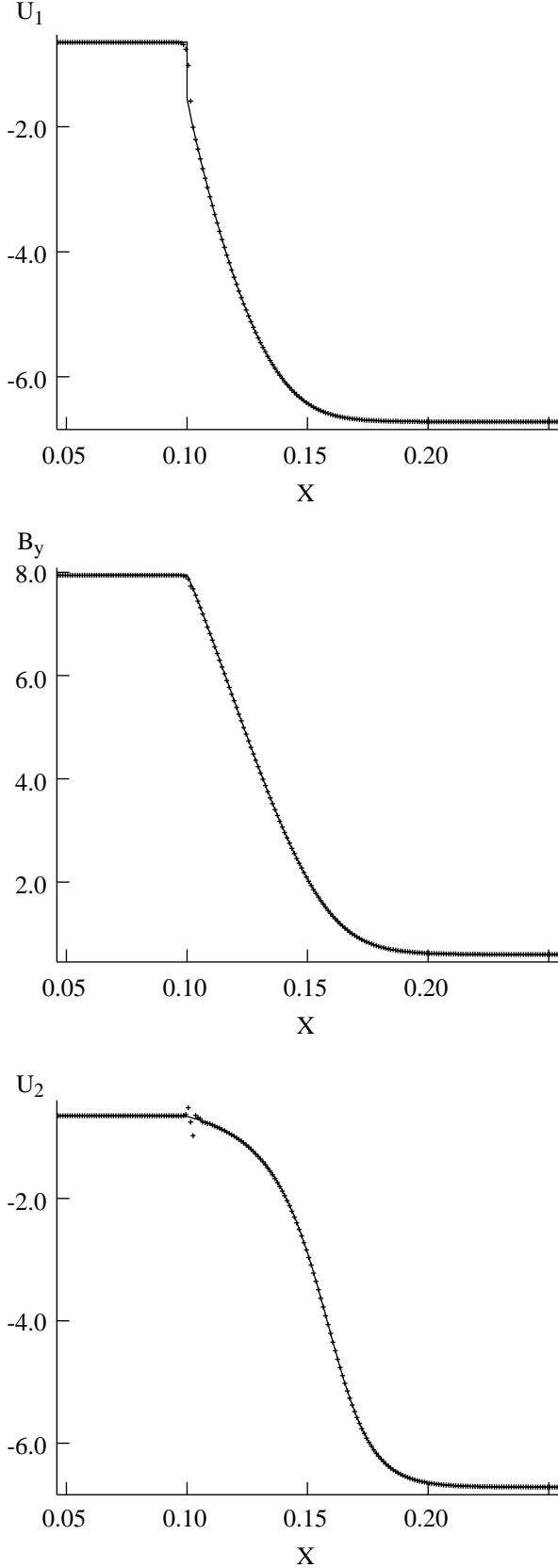


Figure 5. Neutral x velocity, y component of magnetic field and fluid 2 x velocity for case C with $\Delta x = 10^{-3}$. The line is the solution to the steady equations and the markers are the time dependent numerical solution.

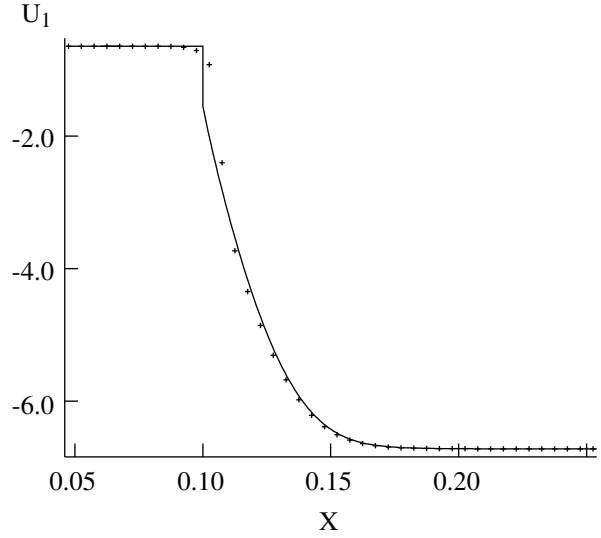


Figure 6. Neutral x velocity for case C with $\Delta x = 5 \cdot 10^{-3}$. The line is the solution to the steady equations and the markers are the time dependent numerical solution.

4.4 Case C (Neutral Sub-shock)

This is similar to case A except that the neutral sound speed $a = 1$ and the upstream fast Mach number $M_f = 5$, which mean that there is a neutral sub-shock at the downstream end of the structure. Fig 5 shows that the agreement between the two solutions is again excellent, except for the finite width of the sub-shock in the solution computed with the time dependent code. There is also an error in the charged fluid x velocities inside the sub-shock, but this does not affect the solution elsewhere. This error arises because of the exact steady solution has a discontinuity in the electric field at the sub-shock and could be reduced by adding viscosity to increase the width of the sub-shock. However, there is little point in doing this since the assumption that the inertia of the charged particles is negligible is not valid within the sub-shock. Note that in this case also, the results are still satisfactory at much lower resolution (Fig 6).

Since the neutral x-velocity is discontinuous at the neutral sub-shock, which is smeared out in the numerical solution, we expect the rate of convergence to be first order. In fact, with $x_0 = 0.065$, $x_1 = 0.215$, we get $\epsilon_{u_1} = 6.88 \cdot 10^{-3}$ for $\Delta x = 0.001$ and $\epsilon_{u_1} = 6.98 \cdot 10^{-2}$ for $\Delta x = 0.005$. This gives $\epsilon_{u_1} \propto \Delta x^{1.44}$, which is significantly better than first order. This merely indicates that, at this resolution, the error is not entirely dominated by that at the sub-shock. If we increase the resolution to $\Delta x = 5 \cdot 10^{-4}$, we get $\epsilon_{u_1} = 3.94 \cdot 10^{-3}$ which corresponds to $\epsilon_{u_1} \propto \Delta x^{0.81}$ when compared to $\Delta x = 0.001$. That this is somewhat worse than first order is probably because rounding errors are becoming significant at such high resolution.

5 CONCLUSIONS

It is clear that the code described in this paper is both robust and accurate and it also has the advantage that, unlike

explicit methods, the timestep at high numerical resolution is not restricted by either the Hall or ambi-polar terms. Although this is particularly important when the Hall term dominates over ambi-polar diffusion, it also gives a significant increase in efficiency at high resolution when this is not the case. A code that is efficient at high resolution is necessary if one wishes to study multi-fluid shock structures with a distribution of grain sizes and realistic physics. The fact that a Hall term that is large compared to ambi-polar diffusion imposes such a severe restriction on the timestep for explicit schemes also has important implications for any numerical calculations that include this effect. It may be that at relatively low resolution an explicit scheme is stabilized by the numerical dissipation due to the hyperbolic terms, but such a scheme will require a very small timestep if the resolution is sufficient to give accurate results.

Although we have only described a one dimensional algorithm, its structure is such that is a simple matter to extend it to multi-dimensions. A multi-dimensional version of this code would have numerous applications to the dynamics of molecular clouds in general and star formation in particular. For example, Wardle (1991) has suggested that the instability that affects C-type shocks is generic and is likely to be important whenever there is both ambi-polar diffusion and a dynamically significant magnetic field. It can also be applied to accretion discs, such as proto-planetary discs and those in dwarf novae, in which the high density reduces the ion Hall parameter to the point where both ambi-polar diffusion and the Hall effect are significant (e.g. Sano & Stone 2002).

We have not considered the other source terms such as the ionization and recombination, chemical reactions and radiative cooling, but these terms do not present any obvious difficulty. There may be occasions when they are stiff, but this merely requires locally implicit methods rather than the globally implicit method that we have used for the induction equation.

ACKNOWLEDGEMENTS

The author would like to thank T. W. Hartquist for suggesting this problem and for much helpful advice and criticism. The final version has also benefitted from helpful suggestions from an anonymous referee. The workstations on which these calculations were carried out were funded by PPARC and the steady solutions were computed using Maple.

REFERENCES

- Chieze J.-P., Pineau des Forêts G., Flower D. R., 1998, *MNRAS*, 295, 672
- Chrysostomou A., Burton M. G., Axon D. J., Brand P. W. J. L., Hough J. H., Bland-Hawthorn J., Geballe T. R., 1997, *MNRAS*, 298, 605
- Ciolek G. E., Roberge W. G., 2002, *ApJ*, 567, 947
- Cowling T. G., 1957, *Magnetohydrodynamics*, Interscience, New York
- Draine B. T., 1980, *ApJ*, 241, 1021
- Draine B. T., 1986, *MNRAS*, 220, 133
- Draine B. T., Katz N., 1986a, *ApJ*, 306, 655
- Draine B. T., Katz N., 1986b, *ApJ*, 310, 392
- Draine B. T., McKee C. F., 1993, *Ann. Rev. Astron. Astrophys.*, 31, 373
- Draine B. T., Roberge W. G., 1982, *ApJ*, 259, L91
- Draine B. T., Roberge W. G., Dalgarno A., 1983, *ApJ*, 264, 485
- Chernoff D. F., 1987, *ApJ*, 312, 143
- Chernoff D. F., McKee C. F., Hollerbach D. J., 1982, *ApJ*, 259, L97
- Falle S. A. E. G., 1991, *MNRAS*, 250, 581
- Flower D. R., Pineau des Forêts G., Hartquist T. W., 1985, *MNRAS*, 216, 775
- Hollerbach R., Rüdiger G., 2002, *MNRAS* 337, 216
- Kaufman M. J., Neufeld, D. A., 1996a, *ApJ*, 456, 250
- Kaufman M. J., Neufeld, D. A., 1996b, *ApJ*, 456, 611
- Mac Low M.-M., Smith M. D., 1997, *ApJ*, 491, 596
- Mouschovias T. Ch., 1991, in Lada C. J., Kylafis N. D., eds, *The Physics of Star Formation and Early Stellar Evolution*, Kluwer, p. 449
- Mullan D. J., 1971, *MNRAS*, 153, 145
- Nakano T., Umebayashi T., 1986, *MNRAS*, 218, 663
- Pilipp W., Hartquist T. W., 1994, *MNRAS*, 267, 801
- Pineau des Forêts G., Flower D. R., Hartquist T. W., Dalgarno, A., 1986, *MNRAS*, 220, 801
- Roberge W., Draine B. T., 1990, *ApJ*, 350, 700
- Smith M. D., Brand P. W. J. L., 1990, *MNRAS*, 245, 109
- Smith M. D., Brand P. W. J. L., Moorhouse A., 1991, *MNRAS*, 248, 451
- Smith M. D., Mac Low M.-M., 1997, *A&A*, 326, 801
- Stone J. M., 1997, *ApJ*, 487, 271
- Sano T., Stone J. M., 2002, *ApJ*, 570, 314
- Tóth G., 1994, *ApJ*, 425, 171
- van Leer B., 1977, *J. Comp. Phys.*, 23, 276
- Wardle M., Draine B. T., 1987, *ApJ*, 321, 321
- Wardle M., 1991, *MNRAS*, 251, 119
- Wardle M., 1998, *MNRAS*, 298, 507